Predicting The Capillary Water Absorption Values Of Building Stones By Hybrid Models

Gang Li[1*], Yufei Fu[2], Zixin Deng[1], and Yuan Huang[3]

[1] School of Design and Art, Jiangxi University of Finance and Economics; Nanchang JiangXi, 330032, China
[2] Faculty of Humanities and Arts, Macau University of Science and Technology; Macao 999078, China
[3] Art Institute, Xiangtan University; Xiangtan Hunan, 411105, China
[*] Corresponding author. E-mail: dylan523@163.com

Received: May 14, 2024; Accepted: Aug. 05, 2024

The determination of rock's Capillary water absorption (CWA) requires extensive and complex empirical investigations, while forecasting algorithms could reduce the cost and time required. To achieve this goal, various rock records were collected from different rock types. For the forecasting model, two techniques named ANFIS and SVR were developed, with the model parameters determined using the Imperialist Competitive Algorithm (ICA). The proposed hybrid ICA-SVR and ICA-ANFIS models demonstrate exceptional performance in predicting CWA, with R^2 values exceeding 0.9851 and 0.9586 for the testing and training stages, respectively, indicating a strong correlation between predicted and measured CWA values. Considering all computed metrics, the SVR model optimized with ICA yielded better results than the ICA-ANFIS model in both testing and training stages. For example, the R^2 values for the ICA-SVR model were 0.9758 and 0.9747 for the testing and training datasets, respectively, with VAF values of 0.9889 and 0.9859 . The ICA-ANFIS model also produced acceptable results, though its performance was slightly weaker than the SVR model. Compared to a previous study, the proposed models show a significant improvement in efficiency, with the R^2 value increasing from 0.708 to 0.9889 . In summary, the enhanced ICA-SVR model can be considered a reliable and powerful tool for accurately determining the optimal values of the system's key variables.

Keywords: Capillary water absorption; Building stones; Estimation; imperialist competitive algorithm; ANFIS; SVR

http://dx.doi.org/10.6180/jase.202506_28(6).0013

1. Introduction

Stones have been used as construction materials during the ages. Buildings or monuments made with stone or soil can be affected significantly by water degrading them [1–5]. Capillary water absorption (CWA) forces can impact the underground water and rise through stones. The kinetics of CWA increment provides an indicator for the capability of the materials to degrade parameters [6]. The degradation process can be accelerated by capillary impact, leading to water in some sections of historical constructions and monuments [7]. The absorption of water in porous rocks according to *CWA* impact is the impressive principal degradation procedure. Through this process, the water's movement to a free stage within the porosity of rock can determine the effective CWA power [8]. The CWA properties of rocks have a required impact on the composition, structure, texture, and porousness of rocks [9–12]. Some reports suggested that *CWA* has a useful relevance with porosity [13, 14], and the *CWA* capacity determines the pore size [3, 14, 15].

Nowadays, to decline time and expenses, *AI* adapted with empirical records is applied [16–19]. Within the simple method of regression, the link between CWA with its properties could be considered [13, 20, 21]. The reverse model of P -wave velocity and *CWA* is shown in an analysis. An-

other paper presents that there is a straight connection between *CWA* and resistance [13, 20]. In travertine stones, the *CWA* value gained by testing the water absorbency by weight (W_a) and surface porosity in the simple regression and artificial neural network systems [22] Lately, a study of existing variables has been carried out and a novel relationship was outputted, reporting the best value of R^2 around 0.708 [23]. In order to properly achieve the stones' attributes, the ANN system could be largely applied in civil engineering [24, 25].

Determining the rock's *CWA* requires arduous and hard empirical affairs, while forecast algorithms could decrease the expense and needed time. To reach the aforesaid goal, several rock records were gathered from rocks of different kinds. In order to the forecast outline, ANFIS and SVR models were developed, where the two specification parameters of ANFIS algorithm and the determinative variables' best value of the SVR model were specified by connecting with the imperialist competitive algorithm (ICA), named ICA - SVR and ICAANFIS. The current research recency is that took into account hybrid methods have not been proposed to forecast the rocks' CWA. To expand considered frameworks, the collected collection of data for forecasting *CWA* from the published study was separated into two sections after being accidentally classified.

2. Method

2.1. Data collection

Different samples of stone, including metamorphic, igneous, travertine, etc., were collected from Anatolia and Turkey and studied in a laboratory. These samples were tested in equal sizes of $20 \times 30 \times 30$ cm [23]. These homogeneous samples were tested in the laboratory to obtain CWA values. There are various methods for obtaining variables; in the present section, caliper and satiation methods are used in order to find (W_a) and (n) values. The ρ_d value according to the International Society of Rock Mechanics (ISRM)) standard [26], was obtained by calculating the sample weight's ratio to the mass and cutting the stone from the middle. The E48 Pulse Generator Unit including two transducers (frequency of 54 kHz) [26], was also used to obtain V_p. There are several other methods for calculating *CWA*, one of these is TS EN 19251925 [27]. The test finished when the difference in difference among the two calculated values was less than 1%. The curve drawn slope to show the diversity in values is *CWA*.

The dataset gathered from the study was separated into two parts after being accidentally classified to predict CWA to extend the mentioned models [23]. The collected dataset can be divided into the training and testing stages in various proportions such as 90/10, 85/15, 80/20, 75/25, and 70/30, based on the previously published articles. In the present study, all of these proportions have been analyzed and the best percentage has been selected. For this purpose, with a proportion of 75% and 25%, respectively, the dataset was separated into training and testing data [28]. Important parameters to building stones' forecast *CWA* values, input variables suchlike V_p, ρ_d, n, and W_a, were selected. In the following Fig. 1, and Table 1 the descriptive measures of input and output variables, and their diffusions

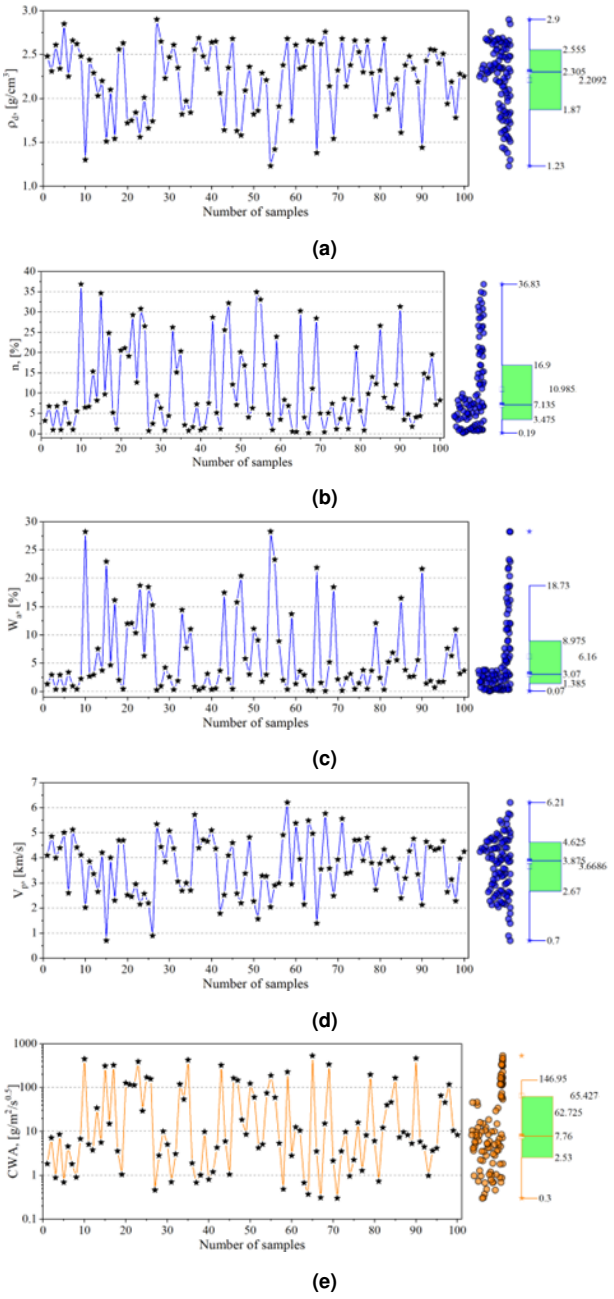

Fig. 1. Distribution of input and output variables

Table 1. Parameters' descriptive statistics used in models

Data Category	Index	Input Variables				Output Variables
		ρ_d	n	W_a	V_p	CWA
		g/cm^3	%	%	Kms	$g/m^2/s^{0.5}$
Training data	Minimum	1.23	0.19	0.07	0.7	0.3
	Maximum	2.9	36.83	28.27	6.21	533.29
	Standard deviation	0.4242	10.78	7.4485	1.2489	123.78
	Skewness	-0.505	0.9139	1.3188	-0.161	2.043
	Kurtosis	-0.8342	-0.47	0.81	-0.743	3.645
	Average	2.2052	11.234	6.449	3.643	70.485
Testing data	Minimum	1.44	0.86	0.32	2.13	0.73
	Maximum	2.68	31.31	21.68	4.81	464.867
	Standard deviation	0.3161	7.5822	5.058	0.7952	98.85
	Skewness	-0.776	1.1714	1.7671	-0.609	3.099
	Kurtosis	0.1577	1.334	3.639	-0.683	12.228
	Average	2.2212	10.241	5.2912	3.746	50.253

were demonstrated, respectively. Table 2 presents the relevance matrix, where the relevance among two parameters is defined by every value. Observing the table, it proposed great negative and positive relevance's among variables, in which the greatest relevance was among ρ_d and n, and among W_a and n at -0.9610 , and 0.9853.

Table 2. Correlation values of parameters

	ρ_d	n	$\mathbf{W}_a$	**V**	CWP
ρ_d	1.0	-0.961	-0.9406	0.8514	-0.7772
n		1.0	0.9853	-0.8194	0.8245
W_a			1.0	-0.7796	0.8403
V_p				1.0	-0.6445
CWP					1.0

2.2. Employed techniques

2.2.1. Imperialist competitive algorithm (ICA)

Atshapaz-Gargari suggested the ICA, human social evolution's simulation in order to dissolve optimization issues [29]. It can decrypt continuous functions with high performance which is recognized as one of the evolution algorithms [30–32]. ICA performs as a global explore algorithm which is expanded based on imperialist contests and social diplomacies [33]. Therefore, the most powerful kingdom can avoid several domains via with their resource. When a kingdom collapses, different other domains can claim with every different to claim the region. The following eight steps can present the ICA kernel. The presented algorithm shows the ICA method's pseudo-code.

a. Made the main kingdom and searched zones accidentally;

b. Territory merger: the realms' position is altered according to the location of countries;

c. Accidentally modifications occur in each country's characteristics as a revolution;

d. Altering the realm's position for the kingdom. A realm with an enhanced position can rise and control the kingdom, and it would replace the prior kingdom;

e. The kingdoms claimed to conquer the different countries;

f. The kingdoms which have less power will be defeated and destroyed. The entire less powerful kingdoms' realms will have been wiped out. According to this step, natural select principles are applied;

g. Check out the stop criteria: if satisfied, stop the competitive process; otherwise, go back to the territory merger step (phase b).

h. Finish.

2.2.2. SVR

Because of the evaluation of certain issues, a support vector machine (SVM) was introduced with the capability of great usages similar to the criterion machine learning proceed [34]. SVM includes two necessary parts, named support vector classification (SVC) and SVR, with SVR commonly used as a standard configuration of SVM [35]. The SVR algorithm's base is for the goal values that reach a $\varphi(x)$ function for designing information to plane area demand to obtain a very flat zone. With help of apperceiving two type of non-linear and linear regressions, discovering answer in order to complexed problems is among them [36]. Linear regression and optimization problems are infeasible to be used by bulging regarding non-linear issues, non-linear regression, and optimization issues by SVR could be used with a bulging computation's optimization through Kernel functions in order to move the information collected in a better dimensional of the information collected in the

particular zone.

2.2.3. ANFIS

ANFIS has known a smooth calculational algorithm that merges neurotic methods with the logic of fuzzy [37]. This organization was generally used in different scopes of engineering [38, 39]. This algorithm can appraise and simulate the planning relevance among dependent and independent variables utilizing a merged training term to specify the most proper fellowship term. The ANFIS's base is the "if - then" rules (Fig. 2). This algorithm includes two steps, a preliminary section and a subsequent section. The inference organization contains five substrates, every of that consists of nodes recognized as node terms. These nodes in the prior substrates released result signals. The function is dispatched an independent signal toward the sub-layer when it retouches the result. In this study, circular and square are as fixed and adaptive nodes were discussed, which can be adjusted to a parameters' set, also shown which they might be entirely refitted in the organization.

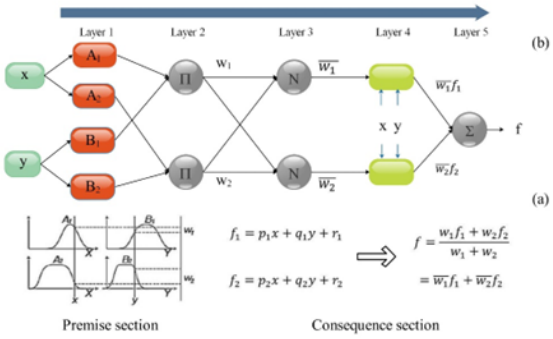

Fig. 2. ANFIS architecture

2.2.4. Hybrid ICA-ANFIS and ICA-SVR

Here, a hybrid SVR model was suggested for the forecasting process. The radial basis function was chosen as the kernel due to the high correlation and the non-linearity properties of the dataset. The main duty in the SVR is indicating the C , sigma, and ε best values. So, the ICA metaheuristic method is selected and connected to the conventional model. Finally, the C, sigma, and ε optimized values concluded as 502.93, 0.4358, and 0.859.

In order to extend the ICA - ANFIS, an initial ANFIS was produced for the start-up stage. The ICA algorithm was then used to optimize the earliest model generated. In this dusty, the membership function characteristics were optimized by the optimization algorithm. Therefore, RMSE was evaluated as a target function. Finally, the optimized ANFIS was generated with the highest iterations and number of fuzzy terms at 25 and 16.

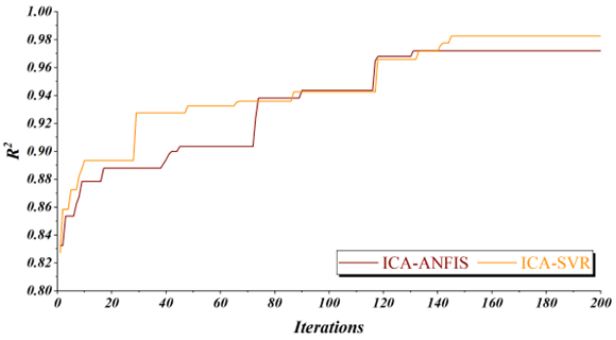

Fig. 3. The fitness curve of the models

The proposed models' performance can be further analyzed by examining the fitness curves, which demonstrate the relationship between the number of iterations and the $R\wedge 2$ value for each model. As shown in Fig. 3, the fitness curve for the ICA - ANFIS model indicates that it converged earlier than the $ICA-SVR$ model, reaching a stable R^2 value after approximately 130 iterations. In contrast, the $ICA-SVR$ model required a slightly longer convergence time, stabilizing its R^2 value after around 150 iterations. The faster convergence of the ICA - ANFIS model can be attributed to the inherent properties of the ANFIS technique, which combines the adaptive capabilities of fuzzy logic and the learning ability of neural networks. The ANFIS model is able to efficiently capture the complex nonlinear relationships between the input parameters and the target CWA values, allowing it to converge more rapidly than the SVR model. However, despite the earlier convergence of the ICA - ANFIS model, the ICA - SVR model ultimately achieved superior performance, as evidenced by the higher R^2 values in both the testing and training stages. This suggests that the SVR model, when optimized using the ICA algorithm, is better able to capture the underlying patterns and relationships within the dataset, leading to more accurate CWA predictions compared to the $ICA-ANFIS$ approach.

2.3. Performance evaluation indices

Determination coefficient (R^2), root mean squared error ($RMSE$), the difference calculated operator (VAF), and mean absolute error (MAE), performance index (PI), inequality index (IA), scatter index (SI), and objective func-

tion (OBJ) were calculated as accurate evaluation:

$$R^2 = \left(\frac{\sum_{p=1}^{P} (t_P - \bar{t})(y_P - \bar{y})}{\sqrt{\left[\sum_{p=1}^{P} (t_P - \bar{t})^2\right]\left[\sum_{p=1}^{P} (y_P - \bar{y})^2\right]}} \right)^2 \quad (1)$$

$$RMSE = \sqrt{\frac{1}{P}\sum_{p=1}^{P} (y_p - t_p)^2} \quad (2)$$

$$MAE = \frac{1}{P}\sum_{p=1}^{P} |y_p - t_p| \quad (3)$$

$$VAF = \left(1 - \frac{\text{var}(t_P - y_P)}{\text{var}(t_P)}\right) * 100 \quad (4)$$

$$PI = \frac{1}{\bar{t}} \frac{RMSE}{\sqrt{R^2 + 1}} \quad (5)$$

$$IA = 1 - \frac{\sum_{p=1}^{P} (t_p - y_p)^2}{\sum_{p=1}^{P} \left(|t_p - \bar{t}| + |y_p - \bar{y}|\right)^2} \quad (6)$$

$$SI = \frac{\sqrt{\left(\frac{1}{P}\right)\sum_{p=1}^{P} \left((t_p - \bar{t}) - (y_p - \bar{y})\right)^2}}{\left(\frac{1}{P}\right)\sum_{p=1}^{P} y_p} \quad (7)$$

$$OBJ = \left(\frac{p}{P} \times \frac{RMSE + MAE}{R^2 + 1}\right)^{\text{Train}} + \left(\frac{p}{P} \times \frac{RMSE + MAE}{R^2 + 1}\right)^{\text{Test}} \quad (8)$$

In these equations, y_P shows the P^{th} pattern forecasted values, t_P shows the P^{th} pattern objective values, $\bar{t}$ stands for the objective values mean, $\bar{y}$ shows the forecasted values mean, and P stands for the dataset's number.

3. Results and discussion

The outcomes of the integrated models for estimating CWA are presented. As mentioned, the two parameters of ANFIS and the parameters' best value in SVR were indicated by emerging with ICA optimization algorithm. The set of data was separated into the training (75 percent) and testing data (25 percent) accidentally. The models' outcomes were analyzed by comparing the measured and estimated values, and the metrics were evaluated, as shown in Table 3 and Fig. 4.

To have a comparing of the usefulness of the hybrid models, four appraiser indices such R^2, RMSE, MAE, and VAF were computed and assessed (Table 3). The concluded outcomes prove that models have considerable workability in the estimation CWA 's procedure with R^2 more than 0.9851 for the training, and 0.9586 for the testing step, explaining the wonderful relevance among observed and estimated CWA. Taking account of the entire criteria, the ICASVR model resulted in proper outcomes compared to ICA - ANFIS. For instance, the R^2, RMSE, MAE, and VAF 's estimated values are 0.9889, 14.69, 8.83, and 98.59 for the

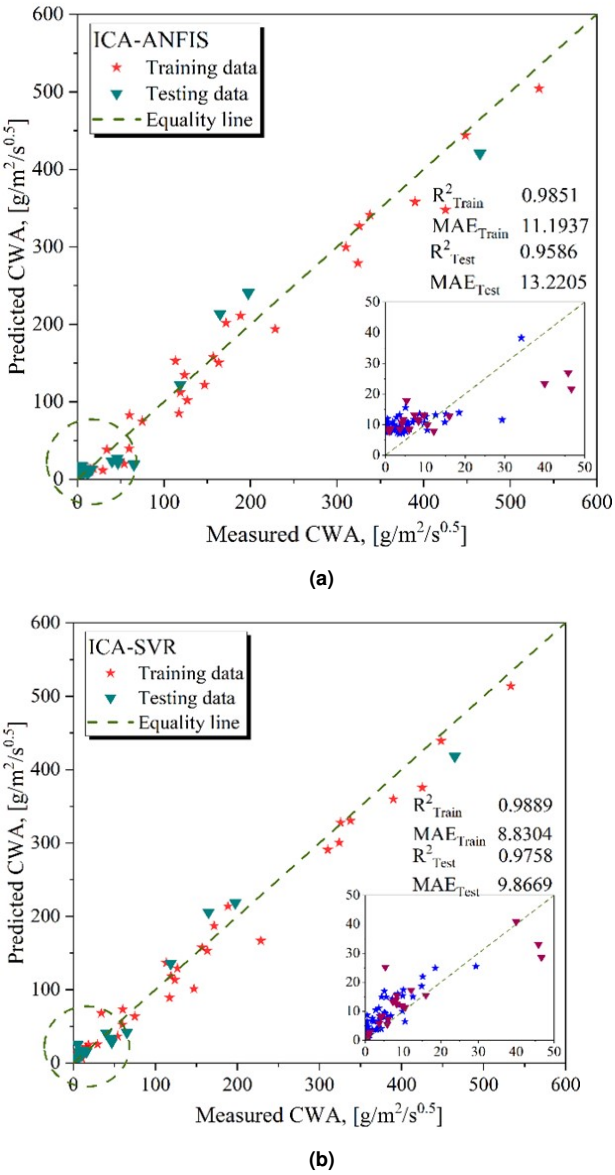

Fig. 4. Simulation results of CWA

$ICA-$ SVR for the training step, and 0.9758, 15.79, 9.867, and 97.47 for the testing step. The ICA ANFIS results are also justifiable; however, its accuracy is roughly less powerful compared to the SVR, with R^2 at 0.9851 and 0.9586, RMSE at 16.889 and 20.13, MAE at 11.19 and 13.22, and VAF at 98.13, 95.85. Also, comparing this study's results with other studies supplies a remarkable enhancement in precision by raising the R^2 0.708 to 0.9889. In conclusion, the created $ICA-SVR$ model might be known as the well-performed framework; this is due to the capability to determine the main model variables' best values.

The supplied Fig. 5 presents the SVR and ANFIS models' performance by presenting the estimated and inves-

Table 3. The performance appraisal values show during testing and steps

Data	Index	ICA-ANFIS	Rank score	ICA-SVR	Rank score	[23]
Train						
	R^2	0.9851	1	0.9889	2	0.708
	RMSE	16.8891	1	14.6935	2	
	MAE	11.1937	1	8.8304	2	
	VAF	98.1383	1	98.5952	2	
	PI	0.1203	1	0.1045	2	
	IA	0.995	1	0.9962	2	
	SI	0.2396	1	0.2085	2	
Test						
	R^2	0.9586	1	0.9758	2	
	RMSE	20.1321	1	15.7945	2	
	MAE	13.2205	1	9.8669	2	
	VAF	95.8547	1	97.4764	2	
	PI	0.2024	1	0.1581	2	
	IA	0.9893	1	0.9933	2	
	SI	0.4006	1	0.3143	2	
Overall	OBJ	14.8673		12.1177		
Summated score			14		28	

tigated CWA, and the histogram plot of residual CWA. Fig. 5 demonstrates the considerable correlation between CWA values. Also, the histogram plots prove that the more normal distribution and cases around zero residual line, the largest accuracy, in which both SVR and ANFIS models have approximately analogous diffusions, while the $ICA-SVR$ specify the most proper outputs.

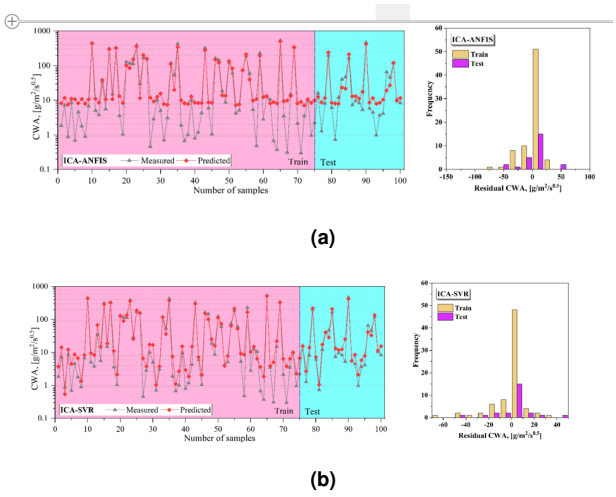

Fig. 5. Results of the models

The results of the FAST (Fourier Amplitude Sensitivity Test) sensitivity analysis are presented in Table 4. The FAST technique was employed to evaluate the relative importance and contribution of the various input variables in determining the target CWA values. As shown in Fig. 3, the FAST sensitivity analysis provides valuable insights into how each input feature influences the model outputs. The results indicate that several input parameters have a significant effect on the CWA values, as evidenced by their high ST (total sensitivity index) values. Specifically, the input parameters with ST values greater than 0.9 were found to have the most considerable influence on the CWA predictions. These include the porosity (n) with an ST value of 0.99566, the P-wave velocity (V_p) with an ST of 0.97424, the water absorption (W_a) with an ST of 0.96191, and the dry density (ρ_d) with an ST of 0.91121. The high ST values for these input parameters suggest that they are the most critical factors in determining the CWA of building stones. This information is crucial for understanding the underlying relationships within the dataset and can help guide future research and modeling efforts. By identifying the key input variables that have the greatest impact on the CWA, the FAST sensitivity analysis provides a clear indication of which parameters should be the primary focus when attempting to optimize or improve the accuracy of CWA predictions. This knowledge can inform the selection of input features, the design of experimental studies, and the development of more robust and reliable forecasting models.

Table 4. FAST sensitivity analysis results

Index	Input variable			
	ρ_d	n	W_a	V_p
ST	0.91121	0.99566	0.96191	0.97424

The performance of the proposed models can be further

evaluated using the Taylor diagram analysis, which provides a comprehensive visualization of the models' ability to accurately predict the target CWA values. The results of the Taylor diagram analysis are presented in Fig. 6, with separate diagrams for the training and testing stages. The Taylor diagram allows for the simultaneous assessment of three key statistical metrics: the standard deviation (SD), the correlation coefficient (R), and the root-mean-square difference (RMSD) between the predicted and observed CWA values. The closer the model's data point is to the reference point (the green dot on the x-axis), the better the model's performance in predicting the CWA. As shown in Fig. 6, for both the training and testing phases, the data point corresponding to the ICA SVR model is located closer to the reference point than the ICA - ANFIS model. This indicates that the ICA-SVR model demonstrates superior performance in terms of accurately predicting the CWA values, with a higher correlation coefficient, lower RMSD, and standard deviation closer to the observed values. The improved performance of the ICA-SVR model can be attributed to its ability to capture the complex nonlinear relationships between the input parameters and the CWA output more effectively than the ICA - ANFIS approach. The Support Vector Regression (SVR) technique, when optimized using the Imperialist Competitive Algorithm (ICA), appears to be better suited for modeling the underlying patterns in the data, leading to more accurate CWA predictions. In contrast, the ICA - ANFIS model, while also demonstrating acceptable performance, is slightly farther from the reference point in the Taylor diagram, indicating a lower correlation, higher RMSD, and greater deviation from the observed CWA values. This suggests that the hybrid ANFIS model, even when optimized with the ICA algorithm, may not be as effective as the ICA SVR model in capturing the nuances of the CWA prediction problem. The insights provided by the Taylor diagram analysis reinforce the findings from the previous sections, further highlighting the superior predictive capability of the $ICA - SVR$ model compared to the ICA - ANFIS approach for the CWA forecasting task.

4. Conclusion

Determining the rocks' capillary water absorption (*CWA*) requires arduous and hard empirical affairs, while forecaster algorithms could decrease the expense and needed time. The integration of the Imperialist Competitive Algorithm (*ICA*) with Adaptive Neuro-Fuzzy Inference System (*ANFIS*) and Support Vector Regression (*SVR*) models significantly enhances the predictive accuracy and efficiency for determining rocks' capillary water absorption (*CWA*).

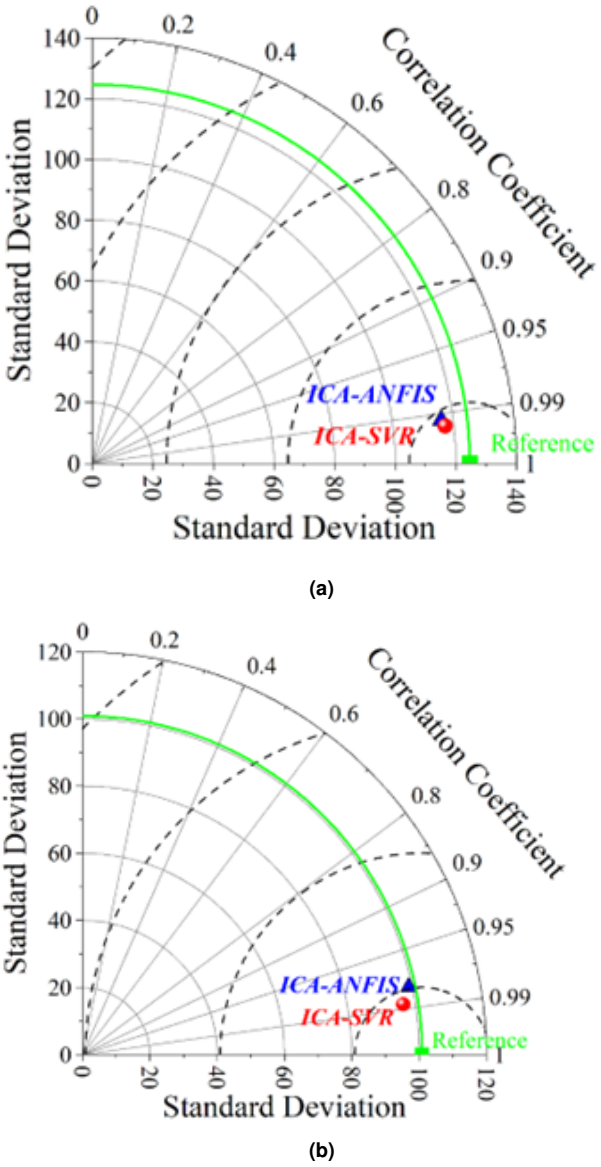

Fig. 6. Results of the models

For the prediction outline, two *ANFIS* and *SVR* analyses were developed, where the *ANFIS* method's two specification parameters and the determinative variables' best value of the *SVR* model were specified by connecting with imperialist competitive algorithm (*ICA*), named *ICA-SVR*, and *ICA-ANFIS*. The principal outcomes are as follows:

- *ICA*-optimized models (*ICA-ANFIS* and *ICA-SVR*) demonstrated superior accuracy in predicting CWA by effectively tuning critical parameters. Both models significantly reduced the time and resources required compared to traditional empirical methods. Also, these models provide a streamlined, accurate, and efficient approach for predicting *CWA*, beneficial

for various engineering and geological applications.

- The success of *ICA-ANFIS* and *ICA-SVR* models illustrate the transformative potential of combining optimization algorithms with machine learning techniques. This approach not only enhances predictive accuracy but also paves the way for broader applications in other complex predictive tasks across different fields. Future research could explore further refinements and applications of these optimized models, potentially revolutionizing how we approach predictive modeling in various scientific and engineering domains.

- The suggested combined *ICA-SVR* and *ICA-ANFIS* models' outcomes to predict the building stones CWA by considering four performance evaluator criteria show that two models have unbelievable efficiency in the CWA's forecast procedure with R^2 larger compared to 0.9851, and 0.9586 in the learn and exam step, defining the significant relevance among recorded and predicted CWA.

- Taking into account the entire computed criteria, the SVR model optimized with ICA resulted in finer outcomes than *ICA-ANFIS* in both testing and training step. For example, the computed R^2, *RMSE*, *MAE*, and *VAF* are 0.9889, 14.69, 8.83, and 98.59 for the *ICA-SVR* for the training phase, and 0.9758, 15.79, 9.867, and 97.47 for the testing portion, respectively. The outcomes of the *ICA-ANFIS* were also reasonable, but its workability was weaker than the *SVR*, with R^2 at 0.9851 and 0.9586, RMSE at 16.889 and 20.13, *MAE* at 11.19 and 13.22, and *VAF* at 98.13 and 95.85, respectively. Moreover, comparing the findings of a present article with the literature presents an incredible enhancement in usefulness by raising the value of R^2 from 0.708 to 0.9889. Overall, the created *ICA-SVR* can be found as the outperformed system.

- The proposed *ICA-SVR* model demonstrated exceptional performance in predicting the CWA of rocks, outperforming the ICA-ANFIS approach. The *ICA-SVR* model achieved R^2 values exceeding 0.98 in both the testing and training stages, indicating a strong correlation between the predicted and measured *CWA* values. The results of the FAST sensitivity analysis and Taylor diagram analysis further confirmed the superiority of the *ICA-SVR* model, which can be considered a reliable and powerful tool for accurately determining the optimal values of the system's key variables.

Appendix. Utilized data in the testing portion

ρ_d	n	W_a	V_p	CWA
2.3	8.68	3.77	3.9	16.04
2.66	1.23	0.46	4.81	1.28
2.29	8.4	3.68	3.8	8.19
1.8	21.33	12.11	2.73	197.44
2.32	5.65	2.41	3.78	6.08
2.68	0.86	0.32	4.34	0.73
1.88	9.84	5.23	3.89	12.15
2.05	13.98	6.83	4	40
2.22	12.3	5.53	3.57	46.68
1.61	26.6	16.49	2.39	164.73
2.38	8.95	3.79	3.19	7.33
2.48	6.5	2.62	4.27	9.68
2.34	6.3	2.69	4.76	8.32
2.19	12.13	5.54	3.35	5.32
1.44	31.31	21.68	2.13	464.867
2.43	3.46	1.43	4.65	5.83
2.56	4.81	1.88	4.44	4.46
2.55	1.77	0.7	4.32	0.98
2.4	4.04	1.69	4.38	3.65
2.51	4.37	1.74	4.67	4.16
1.94	14.84	7.64	2.64	65.18
2.19	13.76	6.29	3.14	45.91
1.78	19.53	10.96	2.28	118.5
2.28	7.16	3.14	3.97	10.52
2.25	8.23	3.66	4.25	8.3

References

[1] E. Hassankhani and M. Esmaeili-Falak, (2024) *"Soil–Structure Interaction for Buried Conduits Influenced by the Coupled Effect of the Protective Layer and Trench Installation"* **Journal of Pipeline Systems Engineering and Practice *15***: 04024012. DOI: https://doi.org/10.1061/JPSEA2.PSENG-1547.

[2] R. S. Benemaran, (2017) *"Experimental and analytical study of pile-stabilized layered slopes"* **Civil engineering, Tabriz university, Tabriz, Thesis**:

[3] M. J. Mosquera, T. Rivas, B. Prieto, and B. Silva, (2000) *"Capillary rise in granitic rocks: interpretation of kinetics on the basis of pore structure"* **Journal of Colloid and Interface Science *222***: 41–45. DOI: https://doi.org/10.1006/jcis.1999.6612.

[4] M. Esmaeili-Falak, H. Katebi, and A. Javadi, (2018) *"Experimental study of the mechanical behavior of frozen soils-A case study of tabriz subway"* **Periodica Polytechnica Civil Engineering *62***: 117–125. DOI: https://doi.org/10.3311/PPci.10960.

[5] R. S. Benemaran, M. Esmaeili-Falak, and M. S. Kordlar, (2024) *"Improvement of recycled aggregate concrete using glass fiber and silica fume"* **Multiscale and Multidisciplinary Modeling, Experiments and Design**

7: 1895–1914. DOI: https://doi.org/10.1007/s41939-023-00313-2.

[6] M. Karoglou, A. Moropoulou, A. Giakoumaki, and M. K. Krokida, (2005) *"Capillary rise kinetics of some building materials"* **Journal of colloid and interface science *284***: 260–264. DOI: https://doi.org/10.1016/j.jcis.2004.09.065.

[7] A. Bozdağ, İ. İnce, A. Bozdağ, M. E. Hatır, M. B. Tosunlar, and M. Korkanç, (2020) *"An assessment of deterioration in cultural heritage: The unique case of Eflatunpınar Hittite Water Monument in Konya, Turkey"* **Bulletin of Engineering Geology and the Environment *79***: 1185–1197. DOI: https://doi.org/10.1007/s10064-019-01617-9.

[8] S. J. I'anson and W. D. Hoff, (1986) *"Water movement in porous building materials—VIII. Effects of evaporative drying on height of capillary rise equilibrium in walls"* **Building and Environment *21***: 195–200. DOI: https://doi.org/10.1016/0360-1323(86)90030-2.

[9] N. Cueto, D. Benavente, J. Martínez-Martínez, and M. A. García-del-Cura, (2009) *"Rock fabric, pore geometry and mineralogy effects on water transport in fractured dolostones"* **Engineering geology *107***: 1–15. DOI: https://doi.org/10.1016/j.enggeo.2009.03.009.

[10] I. Tomašić, D. Lukić, N. Peček, and A. Kršinić, (2011) *"Dynamics of capillary water absorption in natural stone"* **Bulletin of Engineering Geology and the Environment *70***: 673–680. DOI: https://doi.org/10.1007/s10064-011-0355-x.

[11] İ. Dinçer and M. Bostancı, (2019) *"Capillary water absorption characteristics of some Cappadocian ignimbrites and the role of capillarity on their deterioration"* **Environmental earth sciences *78***: 1–18. DOI: https://doi.org/10.1007/s12665-018-7993-2.

[12] D. Benavente, C. Pla, N. Cueto, S. Galvañ, J. Martínez-Martínez, M. A. García-del-Cura, and S. Ordóñez, (2015) *"Predicting water permeability in sedimentary rocks from capillary imbibition and pore structure"* **Engineering Geology *195***: 301–311.

[13] N. Sengun, S. Demirdag, D. Akbay, I. Ugur, R. Altindag, and A. Akbulut. "Investigation of the relationships between capillary water absorption coefficients and other rock properties of some natural stones, V". In: *Global stone congress*. 2014, 22–25.

[14] H. Stück, S. Siegesmund, and J. Rüdrich, (2011) *"Weathering behaviour and construction suitability of dimension stones from the Drei Gleichen area (Thuringia, Germany)"* **Environmental Earth Sciences *63***: 1763–1786. DOI: 10.1007/s12665-011-1043-7.

[15] İ. İnce, (2021) *"Relationship between capillary water absorption value, capillary water absorption speed, and capillary rise height in pyroclastic rocks"* **Mining, Metallurgy & Exploration *38***(2): 841–853. DOI: 10.1007/s42461-020-00354-y.

[16] M. Esmaeili-Falak and R. S. Benemaran, (2023) *"Ensemble deep learning-based models to predict the resilient modulus of modified base materials subjected to wet-dry cycles"* **Geomechanics and Engineering *32***(6): 583–600. DOI: 10.12989/gae.2023.32.6.583.

[17] M. Esmaeili-Falak and R. Sarkhani Benemaran, (2024) *"Application of optimization-based regression analysis for evaluation of frost durability of recycled aggregate concrete"* **Structural Concrete *25***(1): 716–737. DOI: 10.1002/suco.202300566.

[18] Y. Dawei, Z. Bing, G. Bingbing, G. Xibo, and B. Razzaghzadeh, (2023) *"Predicting the CPT-based pile set-up parameters using HHO-RF and PSO-RF hybrid models"* **Structural Engineering and Mechanics, An Int'l Journal *86***(5): 673–686.

[19] M. Esmaeili-Falak and R. S. Benemaran, (2024) *"Ensemble extreme gradient boosting based models to predict the bearing capacity of micropile group"* **Applied Ocean Research *151***: 104149. DOI: 10.1016/j.apor.2024.104149.

[20] İ. Dinçer, A. Özvan, M. Akın, M. Tapan, and V. Oyan, (2012) *"İgnimbiritlerin kapiler su emme potansiyellerinin değerlendirilmesi: Ahlat Taşı örneği"* **Yüzüncü Yıl Üniversitesi Fen Bilimleri Enstitüsü Dergisi *17***(2): 64–71.

[21] P. Vázquez, F. Alonso, R. Esbert, and J. Ordaz, (2010) *"Ornamental granites: Relationships between p-waves velocity, water capillary absorption and the crack network"* **Construction and Building Materials *24***(12): 2536–2541. DOI: 10.1016/j.conbuildmat.2010.06.002.

[22] İ. Çobanoğlu, (2015) *"Prediction and identification of capillary water absorption capacity of travertine dimension stone"* **Arabian Journal of Geosciences *8***: 10135–10149. DOI: 10.1007/s12517-015-1902-8.

[23] İ. İnce, A. Bozdağ, M. Barstuğan, and M. Fener, (2021) *"Evaluation of the relationship between the physical properties and capillary water absorption values of building stones by regression analysis and artificial neural networks"* **Journal of Building Engineering *42***: 103055. DOI: 10.1016/j.jobe.2021.103055.

[24] M. Esmaeili-Falak, H. Katebi, M. Vadiati, and J. Adamowski, (2019) *"Predicting triaxial compressive strength and Young's modulus of frozen sand using artificial intelligence methods"* **Journal of Cold Regions Engineering *33***(3): 04019007. DOI: 10.1061/(ASCE)CR.1943-5495.0000188.

[25] K. Zhang, Y. Zhang, and B. Razzaghzadeh, (2024) *"Application of the optimal fuzzy-based system on bearing capacity of concrete pile"* **Steel and Composite Structures *51***(1): 25. DOI: 10.12989/scs.2024.51.1.025.

[26] M. G. Culshaw, (2015) *"Ulusay, R (ed.), 2015. The ISRM suggested methods for rock characterization, testing and monitoring: 2007–2014: Cham, Switzerland: Springer."* **Bulletin of Engineering Geology and the Environment *74***: 1499–1500. DOI: DOI10.1007/978-3-319-007713-0.

[27] T. En et al., (2000) *"Natural stone test methods-Determination of water absorption coefficient by capillarity"* **CNR-ICR, Rome**:

[28] R. S. Benemaran and M. Esmaeili-Falak, (2023) *"Predicting the Young's modulus of frozen sand using machine learning approaches: State-of-the-art review"* **Geomechanics and Engineering *34***(5): 507–527. DOI: 10.12989/gae.2023.34.5.507.

[29] E. Atashpaz-Gargari and C. Lucas. "Imperialist competitive algorithm: an algorithm for optimization inspired by imperialistic competition". In: *2007 IEEE congress on evolutionary computation*. Ieee. 2007, 4661–4667. DOI: 10.1109/CEC.2007.4425083.

[30] A. Zadeh Shirazi and Z. Mohammadi, (2017) *"A hybrid intelligent model combining ANN and imperialist competitive algorithm for prediction of corrosion rate in 3C steel under seawater environment"* **Neural Computing and Applications *28***(11): 3455–3464. DOI: 10.1007/s00521-016-2251-6.

[31] M. Elsisi, (2019) *"Design of neural network predictive controller based on imperialist competitive algorithm for automatic voltage regulator"* **Neural Computing and Applications *31***(9): 5017–5027. DOI: 10.1007/s00521-018-03995-9.

[32] S. Hosseini and A. Al Khaled, (2014) *"A survey on the imperialist competitive algorithm metaheuristic: implementation in engineering domain and directions for future research"* **Applied Soft Computing *24***: 1078–1094. DOI: 10.1016/j.asoc.2014.08.024.

[33] L. T. Le, H. Nguyen, J. Dou, and J. Zhou, (2019) *"A comparative study of PSO-ANN, GA-ANN, ICA-ANN, and ABC-ANN in estimating the heating load of buildings' energy efficiency for smart city planning"* **Applied Sciences *9***(13): 2630. DOI: 10.3390/app9132630.

[34] C. Cortes and V. Vapnik, (1995) *"Support-vector networks"* **Machine learning *20***: 273–297. DOI: 10.1007/BF00994018.

[35] H. Nguyen, (2019) *"Support vector regression approach with different kernel functions for predicting blast-induced ground vibration: a case study in an open-pit coal mine of Vietnam"* **SN Applied Sciences *1***(4): 283. DOI: 10.1007/s42452-019-0295-9.

[36] X.-N. Bui, H. Nguyen, H.-A. Le, H.-B. Bui, and N.-H. Do, (2020) *"Prediction of blast-induced air over-pressure in open-pit mine: assessment of different artificial intelligence techniques"* **Natural Resources Research 29**(2): 571–591. DOI: 10.1007/s11053-019-09461-0.

[37] J.-S. Jang, (1993) *"ANFIS: adaptive-network-based fuzzy inference system"* **IEEE transactions on systems, man, and cybernetics *23***(3): 665–685. DOI: 10.1109/21.256541.

[38] B. Sethy, C. Patra, N. Sivakugan, and B. Das, (2017) *"Application of ANN and ANFIS for predicting the ultimate bearing capacity of eccentrically loaded rectangular foundations"* **International Journal of Geosynthetics and Ground Engineering *3***: 1–14. DOI: 10.1007/s40891-017-0112-8.

[39] R. Sahu, C. Patra, N. Sivakugan, and B. Das, (2017) *"Use of ANN and neuro fuzzy model to predict bearing capacity factor of strip footing resting on reinforced sand and subjected to inclined loading"* **International Journal of Geosynthetics and Ground Engineering *3***: 1–15. DOI: 10.1007/s40891-017-0102-x.